Inorganica Chimica Acta, 132 (1987) 197–106

Theoretical and Spectroscopic Studies on Imino-carbon Palladated Pyridine-2-carbaldimines

BRUNO CROCIANI

Istituto di Chimica Generale, University of Palermo, Palermo, Italy

and GAETANO GRANOZZI

Dipartimento di Chimica Inorganica, Metallorganica ed Analitica, University of Padua, Padua, Italy

(Received December 19, 1986)

Abstract

Ab initio LCAO-MO-SCF calculations on the model compounds C_5H_4N-2-$C(R_1)$=NH [R_1 = H (**2c**) and R_1 = *trans*-$PdCl(PH_3)_2$ (**4c**)] indicate that the *E-trans* conformation is favored over the *E-cis* one by 16.9 kJ mol^{-1} for **2c** and by 25.0 kJ mol^{-1} for **4c**. One of the factors which stabilizes the *E-trans* arrangement for **4c** is a weak bonding interaction between the palladium center and the pyridine nitrogen. On going from **2c** to **4c** a slight charge enrichment on the pyridine carbons and a more pronounced one on the nitrogen atoms is computed, whereas the charge density of the imino carbon atom is decreased. In **4c** no π contribution to the Pd–C bond is observed. Protonation of the organic moiety of **4c** in the *E-cis* configuration gives rise to a weak Pd–C π overlap population and to a decreased energy separation between π^*_5(LUMO) and the highest energy occupied π MO(π_4) of the pyridine-2-carbaldimino moiety.

The theoretical results are qualitatively related to structural and spectroscopic data (electronic, IR and ^{13}C NMR) of pyridine-2-carbaldimines and the corresponding imino-carbon palladated derivatives.

Introduction

On the basis of spectroscopic studies, it was reported that uncoordinated α-diimine ligands, such as 1,2-bis(imino)ethanes (**1**) [1], pyridine-2-carbaldimines (**2**) [2] and 2,2′-bipyridine (**3**) [3], assume predominantly a planar or approximately planar *trans* N=C–C=N conformation in solution, with *E*(*anti*) substituents at the imino nitrogen atoms for compounds **1** and **2**:

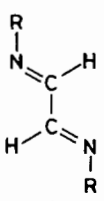

1

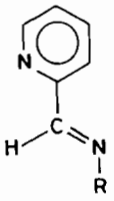

2

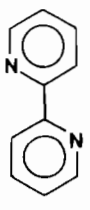

3

The same conformation was observed also in the solid state for CyN=CH–CH=NCy (Cy = cyclohexyl group) [4], C_5H_4N-2-CH=NPh [5], and 2,2′-bipyridine [6] using X-ray diffraction analysis. In accordance with these experimental results, quantum mechanical calculations on compounds **1** and **3** have shown that the planar *E-trans* arrangement is the most stable form [7]. The *E-cis* N=C–C=N conformation, which is assumed when the α-diimine is chelate to a metal center, has a higher potential energy of 26.8 kJ mol^{-1} for **3**, and of 12.5 and 10.5 kJ mol^{-1} for RN=CH–CH=NR (R = H and Me, respectively) [7]. In the latter case, a rotational barrier of 21.7 kJ mol^{-1} (R = H) or 25.5 kJ mol^{-1} (R = Me) is to be overcome for *E-trans* → *E-cis* conversion. In agreement with these theoretical results, the planar *E-trans* conformation is preferentially retained by the 1,2-bis(imino)ethanes (**1**) when they act either as σ,N-monodentate [4] or as σ,σ-N,N′-bridging bidentate ligands [8].

In the course of our investigation on imino-carbon palladated α-diimines, we have prepared complexes of the type $[PdCl\{C(=NR)C(R_1)=NR\}(PPh_3)_2]$ (R_1 = H, Me) [9] and $[PdCl\{C(2\text{-}C_5H_4N)=NR\}(L)_2]$ (L = PPh_3, $PPhMe_2$, PEt_3) with a *trans*-L–Pd–L coordination geometry [10], which exhibit conformational behavior of the α-diimino moiety similar to that of compounds **1** and **2**, both in solution and in the solid state. The X-ray structural analyses of typical representatives of these complexes have shown that the palladated α-diimino group has a virtually planar *trans*-N=C–C=N unit, which lies almost perpendicular to the metal coordination plane [9, 10].

We want to report here an *ab initio* theoretical study carried out on the model compounds C_5H_4N-2-CH=NH (**2c**) and $[PdCl\{C(2\text{-}C_5H_4N)=NH\}(PH_3)_2]$ (**4c**), both with the organic moiety in the *E-trans* and *E-cis* conformations, in order to assess the influence of the metal unit *trans*-$PdCl(PH_3)_2$ on the electronic structure of the pyridine-2-carbaldimino group and on the relative stability of the two conformations. The effect of protonation on the palladated α-diimine is also examined. The theoretical

0020-1693/87/$3.50

results are qualitatively related to the spectroscopic data (electronic, IR and ^{13}C NMR) of pyridine-2-carbaldimines (**2**) and their imino-carbon palladated derivatives (**4–6**):

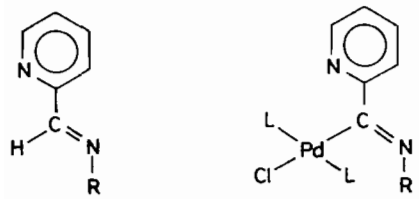

R = C_6H_4OMe-*p*	**2a**	R = C_6H_4OMe-*p*	
R = Me	**2b**	L = PPh_3	**4a**
R = H	**2c**	L = $PPhMe_2$	**5a**
		L = PEt_3	**6a**
R = Me			
L = PPh_3	**4b**	R = H	
L = $PPhMe_2$	**5b**	L = PH_3	**4c**
L = PEt_3	**6b**		

Experimental

Materials and Apparatus

^1H and ^{13}C NMR spectra were obtained on a Varian FT80A spectrometer in CD_2Cl_2 or $CDCl_3$ solution. Infrared spectra were recorded with a Perkin-Elmer 983G instrument, using CaF_2 cells of 0.5 mm width for 1,2-dichloroethane solution in the range 1800–1400 cm^{-1}. The electronic spectra in 1,2-dichloroethane solution were recorded with a Bausch-Lomb Spectronic 210 UV and with a Cary 219 spectrophotometer in the range 550–250 nm at 25 °C, using quartz cells of 1 cm path length.

The pyridine-2-carbaldimines **2a** and **2b** [2] and the imino-carbon palladated derivatives (**4a–6a** and **4b–6b**) [10, 11] were prepared by literature methods. The protonation of **4a** was carried out according to the published procedure [11].

Calculations

The *ab initio* LCAO-MO-SCF calculations were performed by using pseudo-potentials to simulate all core electrons for each atom within the formalism developed by Barthelat *et al.* [12].

Due to the large molecular complexity and the low symmetry, minimal basis sets have been used for ligands, while a double ζ basis set has been optimized for Pd by using a pseudo-potential version of the ATOM program [13]. For the same reason of economy, a further time-saving and quite common approximation [14] was made by assuming the model **4c** where PH_3 replaces the usual phosphine ligands. The calculations were carried out by running the PSHONDO program [15] on a VAX 730 (DEC) computer. The geometrical parameters of **2c** were derived by assuming standard values, whereas those of **4c**(*E-trans*) were obtained from the solid state X-ray structural determination of **5a** [10]. The geometry of **4c** in the *E-cis* conformation has been derived from the *E-trans* one by rotating the pyridine ring and assuming 120° angles around C(1) (see Fig. 1 for atom numbering and axis conventions).

Atomic and bond overlap populations were calculated using Mulliken's scheme [16].

Results and Discussion

Quantum Chemical Calculations

Ab initio results for both *E-trans* and *E-cis* conformations of ligand **2c** are reported in Table I, where energies and percentage atomic populations

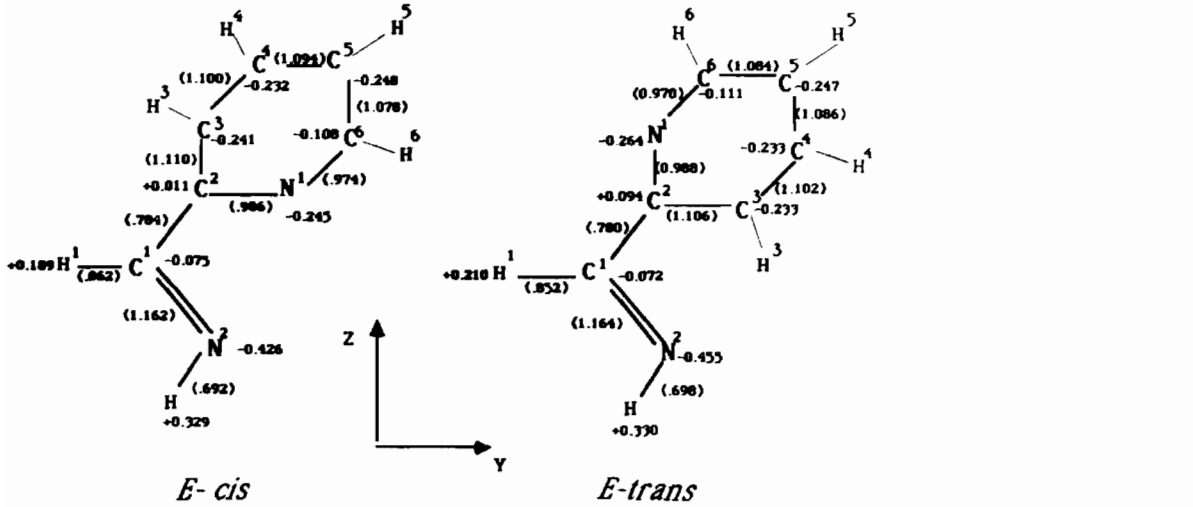

Fig. 1. *Ab initio* gross atomic charges and overlap populations (in parentheses) of *E-trans* and *E-cis* C_5H_4N-2-CH=NH (**2c**).

TABLE I. *Ab initio* Results for *E-trans* and *E-cis* Conformers of **2c**

MO	ϵ (eV)	% Population				Description
		C(1)	N(1)	N(2)	Others	
E-trans						
8a″	9.41	4	15	2	79	π_8^*
7a″	4.81	34	8	27	31	π_7^*
6a″	2.12	0	24	0	76	π_6^*
5a″(LUMO)	1.22	11	10	21	58	π_5^*
4a″(HOMO)	−11.89	6	3	16	75	π_4
16a′	−12.53	4	31	38	27	σ(N(1), N(2))
3a″	−12.59	0	29	0	71	π_3
15a′	−13.18	2	41	37	20	σ(N(1), N(2))
2a″	−14.68	38	0	33	29	π_2
14a′	−16.16	6	8	2	84	σ(ring)
1a″	−17.39	4	18	2	76	π_1
13a′	−17.45	1	13	1	85	σ(ring)
E-cis						
8a″	9.32	4	20	3	73	π_8^*
7a″	4.83	35	0	28	37	π_7^*
6a″	2.02	0	20	0	80	π_6^*
5a″(LUMO)	1.24	10	13	20	57	π_5^*
4a″(HOMO)	−11.91	7	6	17	70	π_4
16a′	−12.57	4	19	58	19	σ(N(2))
3a″	−12.62	0	26	0	74	π_3
15a′	−12.80	2	59	23	16	σ(N(1))
2a″	−14.62	38	0	31	31	π_2
14a′	−16.32	5	8	3	84	σ(ring)
1a″	−17.41	4	17	1	78	π_1
13a′	−17.48	1	12	2	85	σ(ring)

for the outermost occupied and inner virtual molecular orbitals (MOs) are listed.

The *E-trans* arrangement is favored over the *E-cis* one by 16.9 kJ mol^{-1}. Steric repulsion between H(1) and H(3) and electronic repulsion between N(1) and N(2) lone-pairs are certainly responsible of the destabilization of the *E-cis* form. As expected, this value is roughly midway between the corresponding values of molecules **1** and **3** [7]. However, present calculations give a higher rotational barrier (33.9 kJ mol^{-1}) than those reported for **1** and **3** [7]. The computed dipole moments (μ_{cis} = 2.76 D; μ_{trans} = 0.51 D) are sufficiently different to predict some stabilization of the *E-cis* form over the *E-trans* one in polar solvents.

Looking at the valence levels (Table I), only minor energy shifts among the two conformers are present, except for the 15a′ MO which is shifted toward lower energy by 0.38 eV in the *E-trans* form. Together with this shift there is also a change of the atomic composition of 15a′ and 16a′ MOs, *i.e.*, of those orbitals mainly representing the two nitrogen lone-pairs (labelled as σ(N(1), N(2)) in Table I). The explanation of such effects is to be found in a subtle interplay of 'through-bond' and 'through-space' interaction mechanisms [17]. In the *E-trans* conformation only the through-bond mechanism is operating (15a′–16a′ splitting of 0.65 eV) and the two MOs have equivalent localization on the two nitrogen atoms. On the contrary, in the *E-cis* form a destabilization of the inner 15a′ partner is produced by the through-space mechanism (due to negative overlap between the lone pairs) and the two nitrogen lone pairs are more localized (15a′ on N(1) and 16a′ on N(2)). A further consequence of these interactions is the slight charge enrichment of N(1) and N(2) found in the *E-trans* conformation (Fig. 1).

A schematic picture of the π ligand orbitals of the *E-trans* conformer is reported in Fig. 2. A brief discussion of their nature and energy position can be of value for the subsequent analysis of the bonding with the *trans*-PdCl(PH$_3$)$_2$ unit. The π_1, π_3 and π_4 occupied orbitals are mainly localized on the pyridine ring, whereas the π_2 orbital describes predominantly the C(1)=N(2) bond. The pyridine antibonding empty partners are π_5^*, π_6^*, π_8^*, whereas the C(1)=N(2) antibonding MO is π_7^*. The π_4 HOMO appears to be an antibonding combination between π(C(1)=N(2)) and a ring π orbital, whereas the π_5^* LUMO is the bonding combination between the π^*(C(1)=

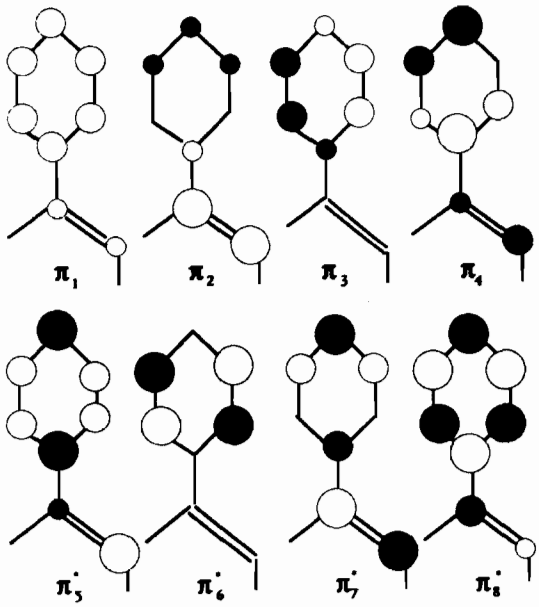

Fig. 2. Schematic picture of the π MOs of *E-trans*-C_5H_4N-2-CH=NH (**2c**).

N(2)) and a ring π^* one. In both cases, however, the localization on the C(1) atom is not high so that a limited amount of π interaction with the metal atom in complex **4c** can be anticipated.

The theoretical results for the *E-trans* and *E-cis* **4c** complexes are reported in Tables II and III, respectively. A correlation diagram between the valence levels of both complexes and corresponding ligands is pictured in Fig. 3.

In agreement with the experimental evidence in the solid state and in solution for the related complexes [10], **4c** is predicted to exist in the *E-trans* form (more stable than the *E-cis* one by 25.0 kJ mol^{-1}). Interestingly, the computed dipole moment of **4c**(*E-trans*) (3.82 D) is much larger than the value of **4c**(*E-cis*) (1.60 D), that is exactly the opposite behavior with respect to the ligand **2c**. Thence, a further stabilization of the *E-trans* form is expected in polar solvents. An accurate analysis of the *ab initio* eigenvectors suggests that a further contribution to the destabilization of the *E-cis* form arises from repulsion between the Pd and H(3) atoms. Actually, the significant polarization of H(3) (Fig. 4) and the negative Pd–H(3) overlap population (–0.078), computed for the *E-cis* form, are both indicative of such a repulsion. On the other hand, a magnetic interaction between H(3) and Pd center in the *E-cis* form is experimentally observable from the large deshielding of the H(3) proton in the ^1H NMR spectrum of the binuclear complex $[ZnCl_2\{C_5H_4N$-2-$C(R_1)$=RN$\}]$ [R_1 = *trans*-$PdCl(PEt_3)_2$; R = C_6H_4-OMe-*p*, which results from the magnetic anisotropy of the d^8 metal center [10].

On the contrary, the present theoretical results suggest that in the *E-trans* conformer an attractive Pd–N(1) interaction is present (see discussion below),

TABLE II. *Ab initio* Results for the *E-trans*-**4c** Complex

MO	ϵ (eV)	% Population								Description[a]
		Pd			Cl	2-PH_3	C(1)	N(1)	N(2)	Others	
		s	p	d							
12a″(LUMO)	1.73	0	0	0	0	0	8	12	15	65	π_5^*
25a′(HOMO)	–8.71	8	8(*y*)	7(z^2)	26(*y*)	5	21	0	18	7	Pd–C(1), Pd–Cl b
24a′	–9.14	0	1	5(*yz*)	94(*z*)	0	0	0	0	0	Cl lp
11a″	–9.18	0	0	2(*xy*)	93(*x*)	5	0	0	0	0	Cl lp
23a′	–9.68	20	0	24(z^2)	43(*y*)	13	0	0	0	0	Pd–Cl b
10a″	–11.30	0	0	3(*xy*)	0	9	10	3	27	48	π_4
22a′	–11.74	0	0	35(x^2-y^2)	15(*y*)	4	2	10	25	9	Pd–Cl b, N(2) lp
9a″	–12.11	0	2	1	2	76	0	6	0	13	PH_3 lp, Pd–P nb
8a″	–12.46	0	0	3(*xz*)	0	0	0	27	1	69	π_3
7a″	–12.77	0	0	90(*xz*)	0	4	0	1	0	5	d_{xz}Pd lp
21a′	–12.87	0	0	47(*yz*)	2	0	1	28	7	25	d_{yz}Pd + N(1) lp
20a′	–12.99	0	0	50(mix)	3	1	1	31	2	12	d Pd + N(1) lp
6a″	–13.49	0	0	43(*xy*)	2	8	10	0	12	25	$\pi_2 + d_{xy}$ ab
19a′	–14.60	4	0	54(z^2, x^2-y^2)	0	41	0	1	0	0	PH_3 lp, Pd–P b
5a″	–14.64	0	0	38(*xy*)	0	17	19	0	13	13	$\pi_2 + d_{xy}$ b
18a′	–15.47	0	0	10(mix)	0	2	21	2	22	43	σ
17a′	–16.17	1	0	6(mix)	1	8	3	7	16	48	σ
16a′	–16.95	0	0	0	0	87	1	1	1	10	$\sigma(PH_3)$
4a″	–16.96	0	0	3	0	37	1	10	0	49	π_1

[a] b = bonding; nb = non bonding; ab = antibonding; lp = lone-pair.

TABLE III. *Ab initio* Results for the *E-cis* **4c** Complex

MO	ε (eV)	% Population									Description[a]
		Pd			Cl	2-PH_3	C(1)	N(1)	N(2)	Others	
		s	p	d							
12a″(LUMO)	1.79	0	0	0	0	0	7	15	15	63	π_5^*
25a′(HOMO)	−8.87	7	8(*y*)	5(z^2)	27(*y*)	4	20	0	22	7	Pd–C(1), Pd–Cl b
24a′	−9.42	0	1(*z*)	5(*yz*)	94(*z*)	0	0	0	0	0	Cl lp
11a″	−9.45	0	0	2(*xy*)	93(*x*)	5	0	0	0	0	Cl lp
23a′	−10.08	22	0	22(z^2)	44(*y*)	12	0	0	0	0	Pd–Cl b
10a″	−11.32	0	0	3(*xy*)	0	6	11	7	27	46	π_4
22a′	−12.00	0	0	40(z^2, x^2-y^2)	14(*y*)	6	0	1	33	6	Pd–Cl b, N(2) lp
9a″	−12.23	0	1(*x*)	1(*xy*)	1	51	0	0	3	43	PH_3 lp, π_3
21a′	−12.32	0	0	4(z^2, x^2-y^2)	0	0	3	69	0	23	N(1) lp
8a″	−12.44	0	1(*x*)	0	1	26	0	22	0	50	PH_3 lp, π_3
7a″	−13.14	0	0	92(*xz*)	0	6	0	0	0	2	d_{xz}Pd lp
20a′	−13.34	0	0	89(*yz*)	4	0	0	3	1	3	d_{yz}Pd lp
6a″	−13.60	0	0	32(*xy*)	2	10	14	0	15	27	$\pi_2 + d_{xy}$ ab
5a″	−14.80	0	0	48(*xy*)	0	18	15	0	9	10	$\pi_2 + d_{xy}$ b
19a′	−14.87	4	0	51(z^2, x^2-y^2)	0	38	0	0	2	5	PH_3 lp, Pd–P b
18a′	−15.56	0	0	14(mix)	1	5	3	5	25	47	σ
17a′	−16.38	1	0	7	0	6	16	2	10	58	σ
4a″	−16.97	0	0	1(*xy*)	0	21	1	14	0	63	π_1
16a′	−17.14	0	0	0	0	40	2	8	3	47	σ

[a] b = bonding; nb = non bonding; ab = antibonding; lp = lone-pair.

in line with the X-ray structural result on **5a** concerning the Pd–C(1)–C(2) bond angle (112.7°) [10], which deviates significantly from the idealized value of 120°. The large charge enrichment of N(1) in **4c**(*E-trans*) (Fig. 4) is probably a consequence of such an interaction.

Let us focus our attention now to the perturbations induced on the pyridine-2-carbaldimino levels by the bonding with the *trans*-$PdCl(PH_3)_2$ metal unit. First of all, we observe a general shift toward higher energies of all π ligand orbitals (Fig. 3) as a consequence of the electron-releasing property of the metal unit. Among π ligand MOs, however, only π_2 is mixed with the Pd d_{xy} orbital, both for energy matching reason and for the large localization of π_2 on the C(1) atom. This mixing gives rise to 5a″(bonding) and 6a″(antibonding) MOs in both *E-trans* and *E-cis* complexes (Tables II and III). Since the LUMO of both complexes is a pure ligand π_5^* orbital, a vanishing Pd–C(1) π bond order is predicted by the present calculations. Actually, the Pd–C(1) overlap population reported in Fig. 4 is completely due to the σ contribution, mostly arising from the 25a′ MO (HOMO of both complexes).

X-ray experimental evidence [10] is in line with this theoretical hint: the observed Pd–C(1) bond length is typical of a single Pd–C(sp^2) bond and no appreciable C(1)–C(2) bond lengthening (expected if the π_5^* orbital is engaged in the bonding) has been detected. However, since the model employed in the present calculations assumes PH_3 instead of PR_3 ligands, we cannot exclude that the charge enrichment of the Pd atom by the more basic phosphine ligands may turn on a certain degree of Pd–C(1) π interaction.

As to the ligand nitrogen lone-pairs, a general shift toward higher energies is observed on going from **2c** to **4c** (Fig. 3). Such a shift is more pronounced for the N(2) than for the N(1) lone-pair. This fact is paralleled by an increase of the N(2) atomic charge in **4c** larger than for N(1), as is clearly seen on comparing the nitrogen atomic charges of Figs. 1 and 4. An increased basicity of the palladated pyridine-2-carbaldimino group can be therefore predicted, in agreement with the well-known enhanced basicity of metallated imino groups [18].

It is also noteworthy to observe the aforementioned mixing between the N(1) lone-pair and metallic 4d orbitals in the **4c**(*E-trans*) (see 20a′ and 21a′ MOs in Table II) which results in a further stabilization of this compound.

Finally, we want to mention briefly an interesting trend that emerges from a calculation carried out on a model of the protonated complex **7c**. The most interesting feature is related to the marked reduction of the Pd–C(1) overlap population (from 0.610 to 0.544) *versus* an increase of the Pd–Cl (0.418) and Pd–P (0.262) overlap populations as a consequence of the changed σ/π capabilities of the protonated group. Looking at the separate contribu-

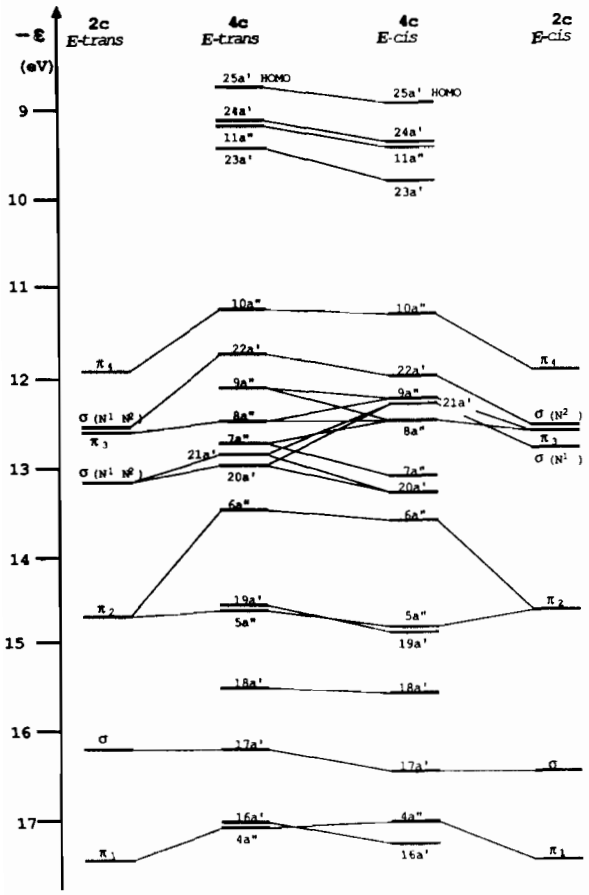

Fig. 3. Correlation diagram between the *ab initio* energy levels of the *E-trans* and the *E-cis* C_5H_4N-2-CH=NH (2c) compounds and their palladated analogs [PdCl{C(2-C_5H_4-N)=NH}$(PH_3)_2$] (4c).

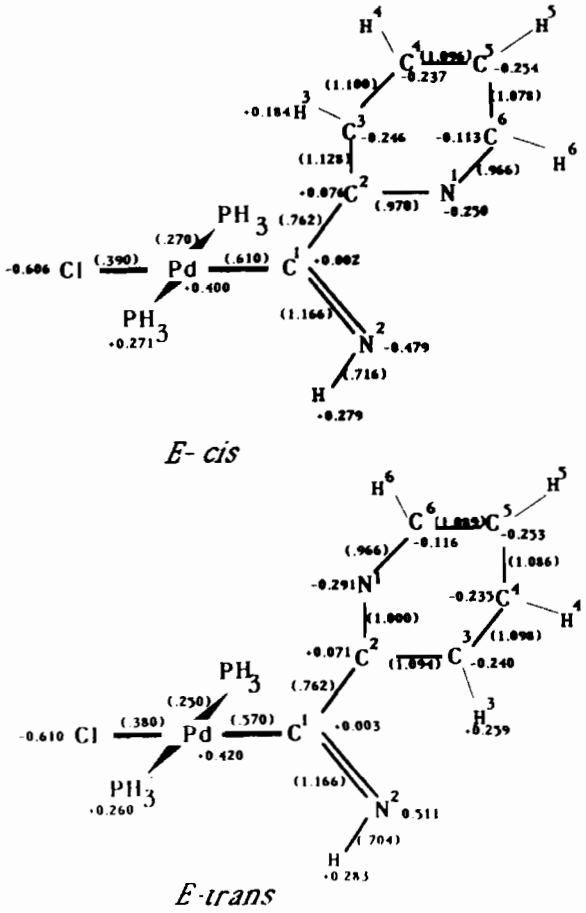

Fig. 4. *Ab initio* gross atomic charges and overlap populations (in parentheses) of [PdCl{C(2-C_5H_4N)=NH}$(PH_3)_2$] (4c) complexes.

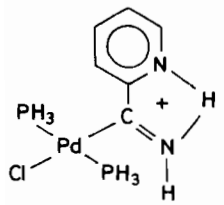

7c

tions to the Pd–C(1) bond, we observe a decreased C(1)--Pd σ interaction (σ overlap population reduced from 0.610 to 0.522) *versus* an increased Pd → C(1) π interaction (π overlap population increased from 0.000 to 0.022), the former effect being largely dominant.

Spectral Data

^{13}C and ^{1}H NMR spectra

The ^{13}C and ^{1}H NMR spectra of the pyridine-2-carbaldimines **2a** and **2b**, and of the PEt_3 complexes **6a** and **6b** are listed in Table IV. The assignments of carbon resonances are based on coupling constant considerations [19, 20] and comparison of ^{13}C chemical shifts with those of related systems [20–22]. In the ^{13}C-{^{1}H} NMR spectra of **6a** and **6b**, the C(2) and N-CH_3 signals appear as triplets due to coupling with the isochronous ^{31}P nuclei of the *trans*-$PdCl(PEt_3)_2$ unit. In agreement with this geometry, a triplet is observed for the PEt_3 methylene carbons. No *J*(CP) coupling is detected for the imino carbon due to the low intensity of this signal.

Replacement of the imino hydrogen of **2a** and **2b** by the *trans*-$PdCl(PEt_3)_2$ group brings about a large downfield shift of *ca.* 30 ppm for the imino carbon C(1). The pyridyl C(2) and the N-C carbons of substituent R are also deshielded by 7–6 and 1–0.4 ppm, respectively, whereas the other pyridyl carbons and the *meta* (C(9, 11)) and *para* (C(10)) carbons of the C_6H_4OMe-*p* group are all slightly shielded (1.4–0.5 ppm). Small shieldings of pyridyl carbons (1.3–0.1 ppm) also occur when the imino nitrogen substituent C_6H_4OMe-*p* of **2a** and **6a** is replaced by the more electron-releasing methyl group of **2b** and **6b**.

TABLE IV. ^{13}C and ^{1}H NMR Data[a]

C_5H_4N-2-C(R_1)=NR		Imino carbon	2-Pyridyl carbons[b]					R Carbons[b]						R_1 Carbons	
R	R_1	C(1)	C(2)	C(3)	C(4)	C(5)	C(6)	N-CH_3	C(7)	C(8,12)	C(9,11)	C(10)	O-CH_3	P-CH_2-	P-CH_2-CH_3
2a C_6H_4OMe-*p*	H	158.5 (163.5)[c]	155.2	121.2 (165.0)[c]	136.5 (164.3)[c] (6.1)[d]	124.8 (164.3)[c] (7.0)[d] (8.4)[e]	149.6 (178.7)[c] (6.8)[d] (3.7)[e]		143.8	122.8 (159.6)[c] (5.8)[d]	114.5 (160.3)[c] (4.9)[d]	159.1	55.5 (143.9)[c]		
6a C_6H_4OMe-*p*	$PdCl(PEt_3)_2$	191.6	162.2 (5.5)[f]	119.8	135.9	123.4	148.3		144.2	123.0	113.8	158.3	55.6	15.7 (12.4)[g]	7.9
2b Me	H	163.4 (161.6)[c] (9.0)[h]	154.9	120.5 (165.0)[c]	136.2 (163.6)[c] (6.2)[d]	124.4 (164.1)[c] (7.0)[d] (8.2)[e]	149.2 (178.3)[c] (6.0)[d] (3.4)[e]	47.2 (134.5)[c] (13.3)[i]							
6b Me	$PdCl(PEt_3)_2$	191.1	160.9 (5.2)[f]	119.4	135.7	123.1	148.2	48.2 (5.3)[f]						15.3 (12.6)[g]	8.1

		Imino proton	2-Pyridyl protons[b]				R Protons[b]			
			H(3)	H(4)	H(5)	H(6)	N-CH_3	H(8,12)	H(9,11)	O-CH_3
2a C_6H_4OMe-*p*	H	8.63	8.19	7.79	7.35	8.69		7.33	6.95	3.83
6a C_6H_4OMe-*p*	$PdCl(PEt_3)_2$		7.91	7.62	7.18	8.58		8.20	6.90	3.80
2b Me	H	8.39	7.96	7.74	7.30	8.64	3.57			
6b Me	$PdCl(PEt_3)_2$		7.69	7.52	7.11	8.50	3.70			

[a] ^{13}C Chemical shifts (ppm, relative to Me_4Si) measured in CD_2Cl_2 solution at 30 °C; coupling constants (Hz) in parentheses; the ^{1}H chemical shifts (ppm, relative to Me_4Si) in $CDCl_3$ solution at 30 °C from ref. 11. [b] Carbon and proton numbering scheme:

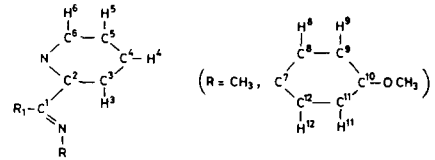

[c] $^{1}J(CH)$. [d] $^{3}J(CH)$. [e] Other long-range $J(CH)$. [f] $^{4}J(CP)$. [g] $^{1}J(PC) + {}^{3}J(P'C)$. [h] $^{3}J(CH)$ with N-CH_3 protons. [i] $^{3}J(CH)$ with imino proton.

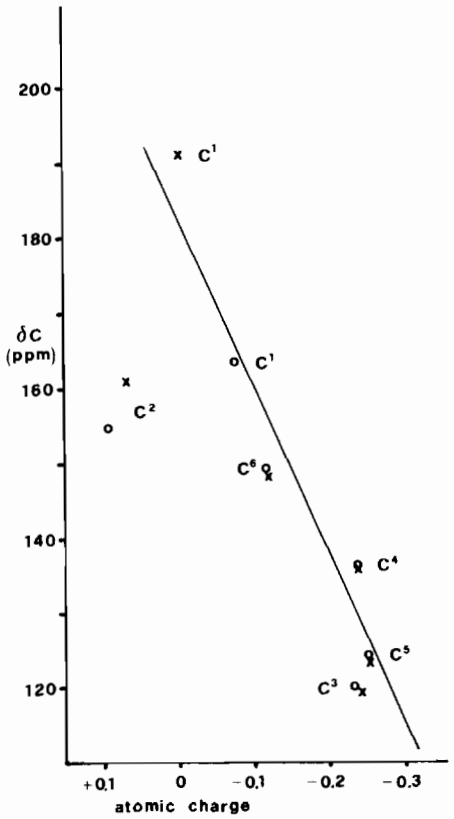

Fig. 5. Observed ^{13}C shieldings for C_4H_4N-2-$C(R_1)$=NR [R = Me, R_1 = H (○); R = Me, R_1 = *trans*-$PdCl(PEt_3)_2$ (×)] *vs.* the calculated carbon total charge for C_5H_4N-2-$C(R_1)$= NH [R_1 = H; R_1 = *trans*-$PdCl(PH_3)_2$].

The ^{13}C NMR chemical shifts are generally correlated with the charge density of the corresponding carbon atoms in a molecule [23]. As is shown in Fig. 5, the observed chemical shifts of imino and pyridyl carbons of compounds **2b** and **6b** decrease almost linearly with increasing charge densities, calculated for the corresponding carbon atoms of the models **2c**(*E-trans*) and **4c**(*E-trans*) respectively, with the exception of the quaternary C(2) carbon. Quite similar behavior is found for the related **2a** and **6a** derivatives. In this context, the slight shielding of C(3), C(4), C(5), and C(6) atoms in the palladated compounds **6a** and **6b**, compared to the pyridine-2-carbaldimines **2a** and **2b**, can be attributed to a slightly increased electron density on the pyridyl ring, promoted by the *trans*-$PdCl(PEt_3)_2$ imino carbon substituent. Consistently, the H(3), H(4), H(5), and H(6) pyridyl protons of **6a** and **6b** resonate at higher field (0.3–0.1 ppm), relative to the corresponding protons of **2a** and **2b** (see Table IV).

Other deshielding factors, such as the magnetic anisotropy of metal d orbitals and, possibly, a certain degree of $d_{Pd} \rightarrow \pi^*_{imino}$ back-bonding may also contribute to the marked downfield shifts of C(1) in **6a** and **6b**, in addition to the reduced charge density indicated by the calculations (see Figs. 1 and 4). On the other hand, the magnetic anisotropy of the d^8 Pd center is largely responsible for deshielding of the closely located N-CH_3 carbon in **6b**, the latter effect being paralleled by the lowfield shift (0.13 ppm) of N-CH_3 proton resonance in the ^1H NMR spectrum of **6b** relative to that of **2b**. The deshielding of C(2) in **6a** and **6b** could also arise from the large through-space Pd---C(2) antibonding interaction computed by the theoretical calculations (overlap population −0.246).

TABLE V. Electronic Spectra[a] and Selected IR Data[b]

Compound	$\pi \rightarrow \pi^*$ (nm)		ν(C=N) (cm^{-1})
2a	286 (10700)	339 (13000)	1626
4a	272sh	331sh	1572
5a	259sh	313sh	1565
6a	<250	296sh	1552
2b		272 (4710)	1651
4b		267 (26700)	1617
5b		257 (25800)	1609
6b		<250	1602
7a	309 (25800)	368 (12800)	

[a]In 1,2-dichloroethane solution at 25 °C; molar extinction coefficients (ϵ (dm^3 mol^{-1} cm^{-1})) in parentheses; sh = shoulder. [b]In 1,2-dichloromethane solution.

Electronic spectra

The absorption maxima of the electronic spectra of pyridine-2-carbaldimines (**2**) and their imino-carbon palladated derivatives (**4**–**6**) are reported in Table V. Due to the well-known limitations of the one-electron picture in reproducing electronic transition energies, no attempt will be made to correlate quantitatively the experimental data to the computed eigenvalues for **2c** and **4c**.

As in the case of the related α-diimino ligands, such as 2,2′-bipyridine **3** [24] and 1,2-bis(imino)-ethanes **1** (R = aryl) [25], the electronic spectrum of **2a**, in the range 450–250 nm, is characterized by $\pi \rightarrow \pi^*$ transitions which give rise to two intense absorption maxima at 339 and 286 nm (Table V and Fig. 6). The progressive red-shift of the lower-energy $\pi \rightarrow \pi^*$ band on going from **3** to **2a** and to **1** (R = C_6H_4OMe-*p*) parallels the progressive decrease in energy of the LUMO in these molecules, as suggested by NDDO calculations on their planar *cis* conformations [26]. In line with theoretical and experimental results [26, 27], the $\pi \rightarrow \pi^*$ transitions become more energetic when the aryl C_6H_4OMe-*p* substituent of **2a** is replaced by the methyl group of **2b**, as a con-

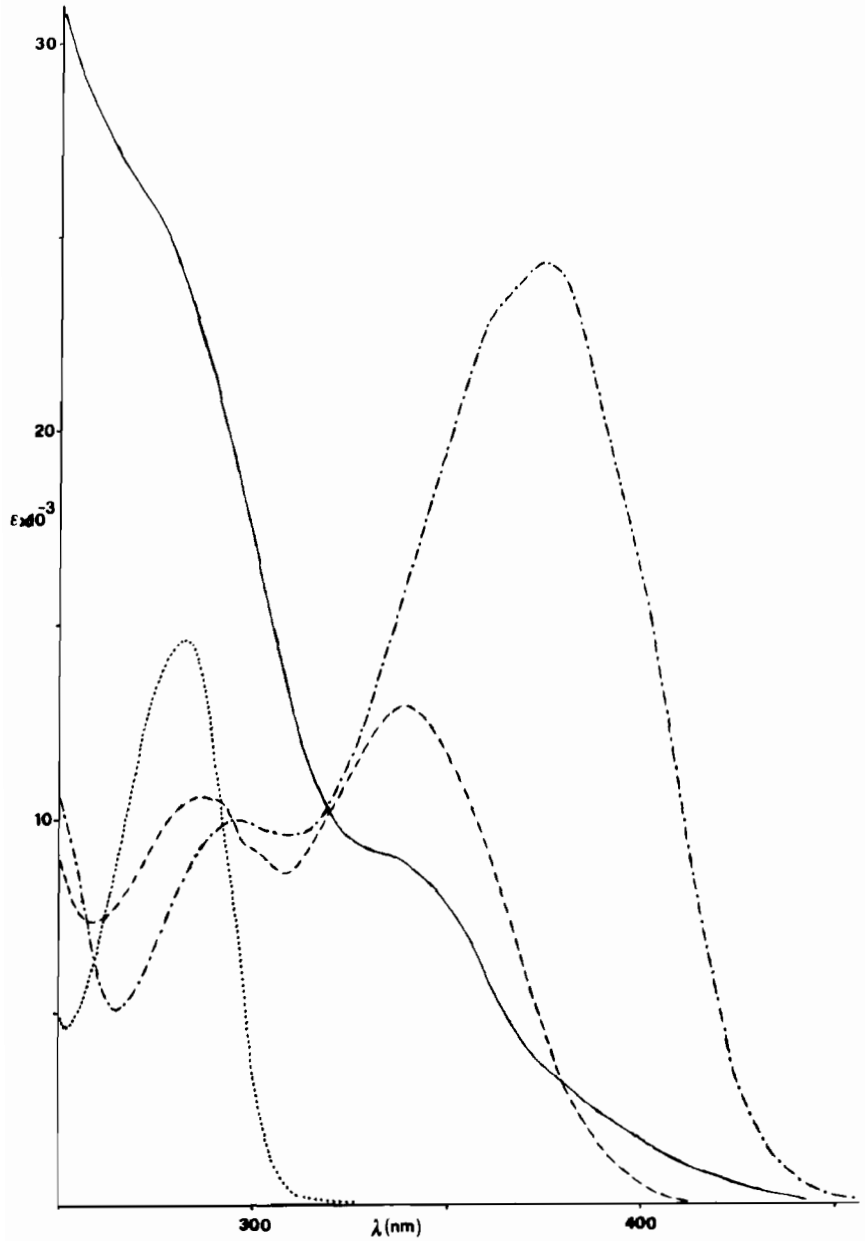

Fig. 6. Electronic spectra of **1**, R = C_6H_4OMe-*p* (– · –), **2a** (– – –), **3** (- - -) and **4a** (——) in 1,2-dichloroethane, at 25 °C in the range 500–250 nm.

sequence of loss of π conjugation and increased inductive effect in the N-CH_3 derivative. For **2b**, only one band is actually observed at 272 nm.

For complexes **4**–**6**, the detection of $\pi \rightarrow \pi^*$ of the imino-carbon palladated moieties is complicated by the strong absorptions of the *trans*-$PdCl(L)_2$ unit, which tail considerably above 250 nm, and possibly by the presence of $d_{Pd} \rightarrow \pi^*_{imino}$ and $\sigma_{Pd-C} \rightarrow \pi^*_{imino}$ transitions in the examined spectral region. However, a plausible assignment can be attempted (as reported in Table V) on the basis of spectral comparison (see, for example, the spectra of **2a** and **4a** in Fig. 6), and of the protonation effect.

Inspection of Table V shows that the electronic bands of the palladated compounds undergo an increasing blue-shift with increasing electron-donor properties of the phosphine L, in the order $PEt_3 > PMe_2Ph > PPh_3$, with a concomitant shift of the imino ν(C=N) band to lower frequencies in the infrared spectrum. The observed trend suggests a small contribution of $d_{Pd} \rightarrow \pi^*$ back-donation to the Pd–C(1) bond, which would bring about an increas-

ing destabilization of the ligand π_5^* orbital (C=N antibonding, see Fig. 2), and a decreasing C=N bond order.

The protonation of **4a** [11] yields the cationic complex **7a** according to eqn. 1.

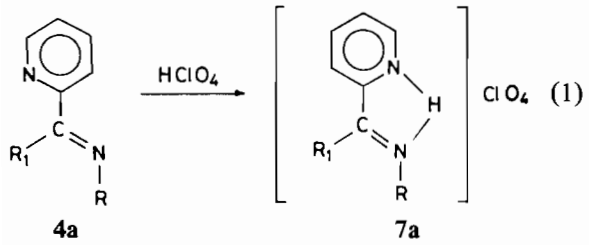

4a **7a**

R = C_6H_4OMe-*p*
R_1 = $PdCl(PPh_3)_2$

The electrophilic attack by the proton does not occur at the Pd–C bond (where the HOMO is essentially localized in the model compound **4c**), but involves the nitrogen lone-pairs with a *trans* → *cis* conformational change of the α-diimino moiety, analogous to that occurring in the σ,σ-N,N′ chelation to transition metal ions [10, 11]. The electronic spectrum of **7a** exhibits two strong $\pi \rightarrow \pi^*$ absorptions at 368 and 309 nm, respectively, at lower frequencies than those of the unprotonated **4a** complex (see Table V). Similar low-frequency shifts of $\pi \rightarrow \pi^*$ transitions were observed in the monoprotonation and σ,σ-N,N′ chelation to transition metal ions of ligands **1** and **3** [24, 25, 28, 29]. Our theoretical results are in qualitative agreement with the observed shifts of $\pi \rightarrow \pi^*$ transitions upon protonation, as the energy separation between π_5^* (LUMO) and the highest energy occupied π MO(π_4) decreases from 13.03 eV in **4c**(*E-trans*) to 11.60 eV in **7c**.

Acknowledgements

Financial support from the Ministero della Pubblica Istruzione (Research Fund 40%) and from CNR (grant no. 85.01467.03) are gratefully acknowledged.

References

1 J. M. Kliegman and R. K. Barnes, *Tetrahedron Lett., 24*, 1953 (1969); H. tom Dieck and I. W. Renk, *Chem. Ber., 104*, 92 (1971); H. tom Dieck and K. D. Franz, *Angew. Chem., 87*, 244 (1975).
2 G. Matsubayashi, M. Okunaka and T. Tanaka, *J. Organomet. Chem., 56*, 215 (1973).
3 K. Nakamoto, *J. Phys. Chem., 64*, 1420 (1960); S. Castellano, H. Gunther and S. Ebersole, *J. Phys. Chem., 69*, 4166 (1965); T. McL. Spotswood and C. I. Tanzer, *Aust. J. Chem., 20*, 1227 (1967).
4 J. Keijsper, H. van der Poel, L. H. Polm, G. van Koten, K. Vrieze, P. F. A. B. Seignette, R. Verenhorst and C. Stam, *Polyhedron, 2*, 1111 (1983).
5 M. Wiebcke and D. Mootz, *Acta Crystallogr., Sect. B, 38*, 2008 (1982).
6 L. L. Merritt and E. D. Schroder, *Acta Crystallogr., 9*, 801 (1956).
7 R. Benedix, P. Birner, F. Birnstock and H. Hennig, *J. Mol. Struct., 51*, 99 (1979).
8 G. van Koten and K. Vrieze, *Adv. Organomet. Chem., 21*, 151 (1982) and refs. therein.
9 B. Crociani, G. Bandoli and D. A. Clemente, *J. Organomet. Chem., 184*, 269 (1980) and refs. therein; B. Crociani, A. Mantovani and A. Scrivanti, *J. Organomet. Chem., 233*, 387 (1982).
10 B. Crociani, M. Sala, A. Polo and G. Bombieri, *Organometallics, 5*, 1369 (1986).
11 B. Crociani, F. Di Bianca, R. Bertani and C. Bisi Castellani, *Inorg. Chim. Acta, 101*, 161 (1985).
12 J. C. Barthelat, P. Durand and A. Serafini, *Mol. Phys., 33*, 159 (1977).
13 B. Ros, C. Salez, A. Veillard and E. Clementi, *Technical Report no. RJ518*, IBM Research, 1968.
14 G. Zangrande, G. Granozzi, M. Casarin, J. P. Daudey and D. Minniti, *Inorg. Chem., 25*, 2872 (1986).
15 M. Dupuis, J. Rys and H. F. King, *J. Chem. Phys., 65*, 111 (1976).
16 R. S. Mulliken, *J. Chem. Phys., 23*, 1823 (1955).
17 R. Hoffmann, *Acc. Chem. Res., 4*, 1 (1971).
18 P. M. Treichel, *Adv. Organomet. Chem., 11*, 21 (1973); D. F. Christian, H. C. Clark and R. F. Stepaniak, *J. Organomet. Chem., 112*, 227 (1976); K. Isobe, E. Kai, Y. Nakamura, K. Nishimoto, T. Miwa, S. Kawaguchi, K. Kinoshita and K. Nakatsu, *J. Am. Chem. Soc., 102*, 2475 (1980).
19 Y. Takeuchi, *Org. Magn. Reson., 7*, 181 (1975).
20 E. Denecke, K. Muller and T. Bluhm, *Org. Magn. Reson., 18*, 68 (1982).
21 T. Drakenberg, *J. Chem. Soc., Perkin Trans. 2*, 147 (1976).
22 W. Danchura, R. E. Wasylishen, J. Delicatny and M. R. Graham, *Can. J. Chem., 57*, 2135 (1979).
23 J. B. Stothers, 'Carbon-13 NMR Spectroscopy', Academic Press, New York, 1972.
24 W. R. McWhinnie and J. D. Miller, *Adv. Inorg. Chem. Radiochem., 12*, 135 (1969).
25 R. W. Balk, D. J. Stufkens and A. Oskam, *J. Chem. Soc., Dalton Trans.*, 1124 (1981).
26 J. Reinhold, R. Benedix, P. Birner and H. Hennig, *Inorg. Chim. Acta, 33*, 209 (1979).
27 H. tom Dieck and I. W. Renk, *Chem. Ber., 104*, 110 (1971).
28 P. M. Gidney, R. D. Gillard and B. T. Heaton, *J. Chem. Soc., Dalton Trans.*, 132 (1973).
29 R. W. Balk, D. J. Stufkens and A. Oskam, *J. Chem. Soc., Dalton Trans.*, 275 (1982).